Eur. Phys. J. B **19**, 409–415 (2001)

THE EUROPEAN PHYSICAL JOURNAL B

EDP Sciences

Isotope effect for transport and magnetic properties of $La_{0.35}Pr_{0.35}Ca_{0.3}MnO_3$ thin films

N.A. Babushkina[1,a], L.M. Belova[1], E.A. Chistotina[1], O.Yu. Gorbenko[2], A.R. Kaul[2], B. Güttler[3], and K.I. Kugel[4]

[1] Russian Research Center "Kurchatov Institute", Kurchatov sqr. 1, Moscow 123182, Russia
[2] Department of Chemistry, Moscow State University, Vorobievy Gory, Moscow 119899, Russia
[3] Physikalisch-Technische Bundesanstalt, Bundesallee 100, 38116 Braunschweig, Germany
[4] Institute for Theoretical and Applied Electrodynamics, Russian Academy of Sciences, Izhorskaya str. 13/19, Moscow 127412, Russia

Received 11 February 2000 and Received in final form 13 September 2000

Abstract. The effect of $^{16}O \rightarrow {}^{18}O$ isotope substitution on electrical resistivity, magnetoresistance, and ac magnetic susceptibility was studied for $La_{0.35}Pr_{0.35}Ca_{0.3}MnO_3$ epitaxial thin films deposited onto $LaAlO_3$ and $SrTiO_3$ substrates. For the films on $LaAlO_3$, the isotope substitution resulted in the reversible transition from a metal-like to insulating state. The applied magnetic field ($H \geq 2$ T) transformed the sample with ^{18}O back to the metallic state. The films on $SrTiO_3$ remained metallic at low temperatures for both ^{16}O and ^{18}O, but the shift of the resistivity peak corresponding to onset of metallic state exceeded 63 K after $^{16}O \rightarrow {}^{18}O$ substitution. The temperature dependence of both resistivity and magnetic susceptibility was characterized by hysteresis, especially pronounced in the case of the films on $LaAlO_3$. Such a behavior gives certain indications of the phase separation characteristic of interplay between ferromagnetism and charge ordering.

PACS. 75.30.Vn Colossal magnetoresistance – 73.50.Jt Galvanomagnetic and other magnetotransport effects (including thermomagnetic effects) – 31.30.Gs Hyperfine interactions and isotope effects, Jahn-Teller effect

1 Introduction

Perovskites of the $R_{1-x}M_xMnO_3$ system, where R^{3+} is a rare earth cation, M is a doubly charged cation of large ionic radius, with both R and M occupying A sites of ABO_3 perovskite lattice, attract significant attention of researchers due to the colossal magnetoresistance (CMR) effect observed in such compounds (see review papers [1,2]). The electron transport in manganites is closely related to spin degrees of freedom through the double exchange mechanism and to the lattice promoting formation of polarons.

Electrical and magnetic properties of manganites are very sensitive to variation of their composition and ambient pressure. Both of these parameters affect tolerance factor $t = d(\text{A-O})/\sqrt{2}d(\text{Mn-O})$, where d denotes an interatomic distance, the former by variation of the mean ionic radii of the cations in A and B positions, the latter due to the different compressibility of A-O and B-O bonds. The tolerance factor value 0.91 was found to be critical for the σ-bonding of the oxygen $2p$ orbitals with e_g orbitals of the Mn ions [3,4]. At lower t, itinerant carriers become localized since O atoms can not facilitate their transport. Localization provides the conditions for charge ordering (Mn^{+3}/Mn^{+4} ordering). The crossover between localized and delocalized states is often accompanied by the phase separation phenomena [5].

The effects of lattice dynamics and local distortions also turned out to be very important [6]. Local Jahn-Teller distortions were revealed by EXAFS and neutron pair-density function (PDF) analysis [7,8] even in the metallic phase. In addition, variation of the Debye-Waller factors for O and Mn atoms [9] accompanying the metal-insulator transition in $R_{1-x}M_xMnO_3$ was found to be more pronounced than the change in the lattice parameters. The results imply that the metal-insulator transition is a lattice dynamics transition at the same time.

All these interrelated phenomena could favor an unusually large isotope effect in manganites first reported in [10]. The isotope effect is most pronounced in the vicinity of the crossover between the charge ordering and metallicity. Isotope exchange in oxygen sublattice, when ^{16}O is replaced by ^{18}O, was found to produce a huge effect on electrical and magnetic properties of certain compounds with tolerance factor $t \approx 0.91$, such as $(La_{1-y}Nd_y)_{0.7}Ca_{0.3}MnO_3$ ($y = 0.5$) [11] and $(La_{1-y}Pr_y)_{0.7}Ca_{0.3}MnO_3$ ($y = 0.75$) [12]. The samples containing ^{16}O being metallic below the Curie temperature T_c became insulating if ^{16}O was replaced by ^{18}O.

[a] e-mail: babushkina@imp.kiae.ru

This metal-insulator transition induced by the isotope substitution was interpreted in [13] as an indication of enhanced electron-lattice interaction near the phase boundary between charge ordered antiferromagnetic and ferromagnetic metal states. This conclusion is supported by the experimental data on the isotope effect in the charge ordering transition [14]. The magnetic susceptibility measurements [15] and neutron diffraction studies [16] demonstrated the importance of phase separation for enhancement of isotope effect near this phase boundary.

Until now the isotope effect has been studied mostly in the bulk samples of manganites. The first results concerning the isotope effect in manganite thin films can be found in several recent publications [17–19]. Epitaxial thin films are very interesting objects for the study of isotope effect. First, their good crystallinity comparable to that of high-quality single crystals provides an opportunity to study the intrinsic properties of the material and eliminate spurious effects related to grain boundaries. Second, the film-substrate lattice mismatch producing epitaxial strain in the film adds new features to the isotope effect in the perovskite materials. The perovskite cell in the film is deformed, compared to the bulk material, to match the atomic positions of the substrate lattice. The remarkable feature of the manganite epitaxial films is that the strain is sustained even if the film thickness exceeds the perovskite lattice constant by a factor of 1000. Such films were grown by a variety of the vapor deposition techniques [20,21]. The strain in the films affects their electrical and magnetic properties as well. In [17] the effect of strains was demonstrated for structural properties and electrical resistivity of isotope substituted $(La_{1-y}Pr_y)_{0.7}Ca_{0.3}MnO_3$ films with $y = 0.5$. Here the first report the influence of magnetic field on the isotope effect in this films and present the measurements of magnetoresistance and ac magnetic susceptibility. We demonstrate that the variation in the lattice strains induced by the substrates results in the striking difference in the magnetoresistance in the phase-separation behavior.

2 Experimental

Aerosol MOCVD used to prepare thin films includes deposition from the vapor produced by evaporation of precursor solution nebula in the carrier gas flow [22]. Volatile precursors were as follows: $La(thd)_3$, $Pr(thd)_3$, $Sr(thd)_2$, $Ca(thd)_2$, and $Mn(thd)_3$, where thd is 2,2,6,6-tetramethylheptan-3,5-dionate. Single crystals of $LaAlO_3$ (pseudocubic cell) and (001) $SrTiO_3$ were used as substrates. Deposition runs were carried out at 750 °C with total pressure of Ar-O_2 mixture 6 mbar (O_2 partial pressure 3 mbar). The prepared $La_{0.35}Pr_{0.35}Ca_{0.3}MnO_3$ films were 60 nm thick. Directly after the deposition at 750 °C, the reactor was filled with oxygen up to the pressure of 1 bar and as-grown films were annealed for 0.5 h at the deposition temperature. SEM was accomplished by CAMSCAN equipped with EDAX system for quantitative chemical analysis of the films. SNMS depth profiling for metal components and ^{18}O was carried out with INA-3 system. XRD with four-circle diffractometer Siemens D5000 with secondary graphite monochromator (Cu K_α radiation) was used to determine phase composition, orientation and lattice parameters. The $\theta - 2\theta$ (including measurements of the tilted samples over the reflection poles found by φ- and χ-scanning), φ scans, and out-of-plane rocking curve measurements were used. Reflections of the substrates were used as an inner standard. Calculations were made with reference to the lattice constants 0.3905 nm for $SrTiO_3$, 0.3792 nm for $LaAlO_3$. The XRD study was repeated after the isotope exchange experiments.

Table 1. Structural characteristics of the $La_{0.35}Pr_{0.35}Ca_{0.3}MnO_3$ films on the perovskite substrates.

Substrate	Lattice parameters[a] (Å)		Tetragonal distortion[b] (%)
	$a/2$, $b/2$	$c/2$	
$LaAlO_3$	3.846 ± 0.003	3.872 ± 0.002	0.7
$SrTiO_3$	3.879 ± 0.003	3.823 ± 0.002	−1.5

[a] Parameters are scaled to the perovskite cell dimension.
[b] Calculated from $[2(c-a)/(c+a)] \times 100\%$.

For isotope exchange, pairs of 1×8 mm^2 strips were cut from the samples and put into platinum boats, which were placed in two quartz tubes mounted in the furnace. The quartz tubes formed parts of two identical closed loops with enforced circulation of gas. All samples were treated simultaneously: one part of the each sample was heated in $^{16}O_2$ atmosphere, the other part of the each sample was heated in $^{18}O_2$ enriched atmosphere (85% molar fraction of $^{18}O_2$). The diffusion annealing was carried out for 4 h at 750 °C under the oxygen pressure of 1 bar.

The oxygen isotope ratio of the films was checked by the Raman spectrometry. The study was performed with a triple monochromator system and in backscattering geometry of the incident laser light.

The electrical resistivity ρ of $La_{0.35}Pr_{0.35}Ca_{0.3}MnO_3$ epitaxial thin films deposited onto $LaAlO_3$ (LAO) and $SrTiO_3$ (STO) substrates was measured by the conventional four-probe technique in the 4.2−300 K temperature range. The measurements of ac magnetic susceptibility $\chi_{ac}(T)$ were performed in ac magnetic field with frequency 3 kHz and amplitude about 4.5 Oe.

3 Results

3.1 XRD characterization

The XRD study revealed that the prepared films were highly strained (Tab. 1). The films were epitaxial (out-of-plane rocking curve FWHM 0.17−0.25 degrees, in-plane orientation defined φ-scans FWHM 0.4−0.8 degrees) with pure cube-on-cube growth mode. The difference of the perovskite lattice constants results in the tetragonal strain of the film lattice in the interface plane. The lattice constant

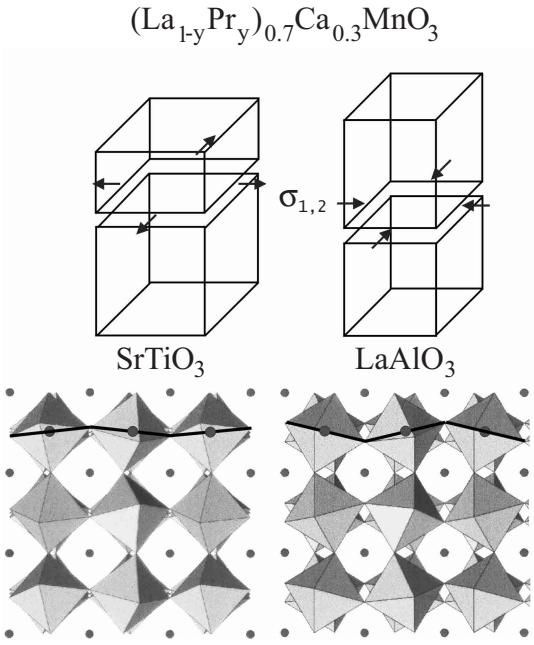

Fig. 1. Perturbation of the intrinsic buckling of the MnO_6 octahedra array under the substrate-induced strains.

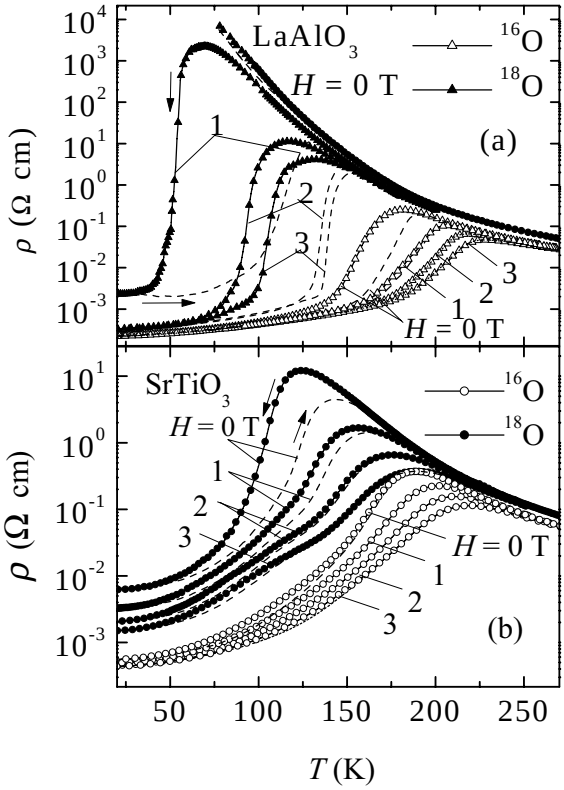

Fig. 2. Temperature dependence of electrical resistivity for $La_{0.35}Pr_{0.35}Ca_{0.3}MnO_3$ films at various magnetic fields: 0 T, 1 T, 2 T, 3 T. (a) films on $LaAlO_3$ substrate, with ^{16}O (open triangles) and ^{18}O (solid triangles); (b) films on $SrTiO_3$ substrate, with ^{16}O (open circles) and ^{18}O (solid circles).

of STO is larger, consequently the tensile strain in the film demands an in-plane expansion of the perovskite cube. For the films on LAO substrates, we have the opposite situation: the lattice constant of the substrate is smaller than that in the manganite film, and this causes in-plane contraction of the films. Deformation of the lattice normal to the substrate is proportional to the in-plane strain components. Thus, the films on STO are contracted along the normal, whereas the films on LAO are stretched. Certainly in this case one can expect a perturbation of the intrinsic buckling of the MnO_6 octahedra array under the strain (Fig. 1).

The high-temperature annealing during the isotope exchange could cause relaxation of the strain. However, the XRD study after isotope exchange did not reveal any appreciable relaxation for the 60 nm thick films used in our experiments. The SNMS depth profiling revealed the complete isotope exchange in our thin-film samples in spite of very slow oxygen diffusion in the nearly stoichiometric $R_{1-y}M_yMnO_3$ owing to the lack of oxygen vacancies [23]. No penetration of ^{18}O into the substrate was detected by SNMS depth profiling.

3.2 Raman spectrometry characterization

All $La_{0.35}Pr_{0.35}Ca_{0.3}MnO_3$ films show the first order Raman active phonon bands with A_g symmetry near 80 cm^{-1}, a doublet structure between 220−290 cm^{-1} and a further band near 440 cm^{-1} with B_g-like character. The bands are superimposed by a strong background scattering with broad peaks near 490 cm^{-1} and 610 cm^{-1} [24]. The bands between 220−290 cm^{-1} and 440 cm^{-1} were unambiguously identified as oxygen bands by isotope exchange experiments. The features near 490 cm^{-1} and 610 cm^{-1} are also of the phonon origin since they also show an oxygen isotope shift. No difference in the band position was registered for the films of the same oxygen composition on LAO and STO.

A significant isotope effect was found for the modes near 240, 440, and 660 cm^{-1}. It corresponds to an $^{18}O/(^{16}O + {}^{18}O)$ ratio of 0.8 ± 0.1. This is in good agreement with the ratio of 0.85 in the exchange gas mixture used in our experiment. The line shift induced by the isotope exchange can be quantitatively related to the mass change involved. This indicates a complete gas exchange. Also, there are no significant contributions from other potential factors resulting from the isotope exchange process such as strain effects or the oxygen nonstoichiometry.

3.3 Electrical resistivity

The $\rho(T)$ curves for the films on LAO and STO substrates annealed both in ^{16}O and ^{18}O are shown in Figure 2. Note that the low value of the resistivity for metal-like films at 4.2 K (about $5 \times 10^{-4}\ \Omega\,cm$) indicates good quality of the films and supports their single-crystalline character. We can see in Figure 2 that the $^{16}O \rightarrow {}^{18}O$ isotope substitution produces different effect on the $\rho(T)$ behavior of the films deposited on LAO and STO. At zero magnetic

field, the film with ^{16}O on LAO exhibits the resistivity peak at $T_p \approx 181$ K with the steep decrease at lower temperatures. Thus, we have the insulator to metal transition in the vicinity of T_p. Resistivity of the film with ^{18}O on LAO behaves in a qualitatively different way: it is growing monotonously when the temperature is lowered. Such an insulator-like behavior is usually attributed to the charge ordering in the manganese sublattice. As a result, we see that the $^{16}O \rightarrow {}^{18}O$ isotope substitution induces the transition from metallic to insulator-like resistivity at low temperatures. We have already observed such a behavior for ceramic $(La_{1-y}Pr_y)_{0.7}Ca_{0.3}MnO_3$ samples at $y = 0.75$ [12]. The behavior of the films on STO remains metal-like at low temperatures even after the isotope substitution, but the resistivity peak shifts from 186 K (^{16}O) to 123 K (^{18}O) at $H = 0$, that is $\Delta T_p = 63$ K.

Measurements were performed for the same samples at applied magnetic fields $H = 1$, 2, and 3 T. The electrical resistivity decreases significantly under effect of magnetic field, and demonstrates metallic behavior at 3 T within a wide temperature range. Magnetic field $H = 1$ T transforms the sample with ^{18}O on LAO from insulating to metallic state with $T_p = 70$ K owing to the suppression of charge ordering. For the samples with ^{16}O on LAO and the samples with ^{16}O and ^{18}O on STO, the applied magnetic field causes a pronounced shift of $\rho(T)$ curves and of T_p toward high temperatures as implied by the double exchange model. The main parameters characterizing the electrical resistance and magnetoresistance for the films under study are presented in Table 2.

The isotope shift of T_p *versus* magnetic field for the films on LAO and STO is illustrated in Table 2. Note that the magnetic field dependence of ΔT_p is more pronounced for the films on LAO having the in-plane compressive stress.

The magnetoresistance $MR = (\rho(0) - \rho(H))/\rho(H)$ ($H = 3$ T) was determined for all samples with ^{16}O and ^{18}O on LAO and STO. The temperature dependence of magnetoresistance for different film samples is shown in Figure 3. The MR is sufficiently large for the films with ^{16}O: $MR = 150$ (the film on LAO) and 10 (the film on STO). The higher value of MR for the film on LAO can be related to the compressive strains induced by the substrate. After the isotope substitution, the MR increases up to 5×10^2 for the film with ^{18}O on STO, whereas for the film with ^{18}O on LAO it is as high as 3.6×10^6. Such a large MR for the film ^{18}O on LAO seems to result from melting of the charge-ordered state in the magnetic field giving rise to a significant resistivity drop.

The $\rho(T)$ curves for all films measured on heating and on cooling exhibit hysteretic behavior. At $H = 0$, it was found that the hysteresis is rather small for the samples on STO annealed in ^{16}O, but it is more pronounced for the samples on LAO. The $^{16}O \rightarrow {}^{18}O$ isotope substitution causes broadening of the hysteresis loops for films on both LAO and STO. The existence of hysteresis suggests the possibility of a phase separation (coexistence of ferromagnetic and antiferromagnetic regions). Such a coexistence was observed by the neutron powder diffraction

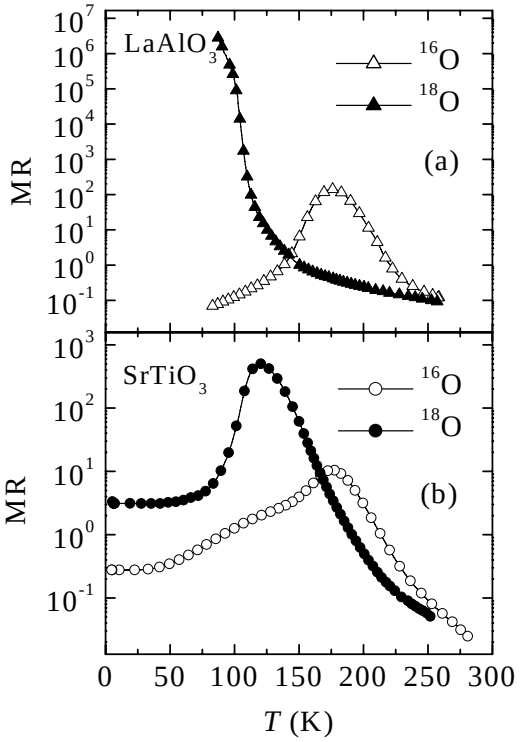

Fig. 3. Temperature dependence of magnetoresistance $MR = \Delta\rho/\rho = (\rho(0) - \rho(H))/\rho(H)$ ($H = 3$ T) for $La_{0.35}Pr_{0.35}Ca_{0.3}MnO_3$ films: (a) on $LaAlO_3$ substrate, with ^{16}O and ^{18}O; (b) on $SrTiO_3$ substrate, with ^{16}O and ^{18}O.

experiments [16] and correlates with the magnetic susceptibility measurements [15] for ceramic and powder samples annealed in ^{16}O and ^{18}O.

At nonzero magnetic fields, the tendency to phase separation should be most clearly pronounced in the samples with ^{18}O on LAO, where the transition to insulating and hence antiferromagnetic phase was observed at $H = 0$. In these films, the applied magnetic field promotes formation of the ferromagnetic phase in addition to the antiferromagnetic one. As a result, we have a pronounced temperature hysteresis of resistivity for the films with ^{18}O on LAO. The cooling curve is shifted toward lower temperatures, and on heating the low-temperature metallic state is apparently frozen, and this causes the shift of the heating curve toward higher T. The width of the hysteresis loop is the largest for this sample at $H = 1$ T. With the growth of magnetic field the potential barrier between antiferromagnetic and ferromagnetic phases lowers, and the hysteresis loops become narrower. The loop width can be used for qualitative evaluation of the role of the phase separation in these films.

The analysis of $\rho(T)$ curves above T_p demonstrates the thermal activation behavior of resistivity. In the paramagnetic range the resistivity can be described by the model of small polaron hopping in the adiabatic regime [25]:

$$\rho(T) = AT \exp(W_p/kT), \quad (1)$$

Table 2. Magnetoresistance of the $La_{0.35}Pr_{0.35}Ca_{0.3}MnO_3$ (LPSM) films on $LaAlO_3$ (LAO) and $SrTiO_3$ (STO) substrates, with ^{16}O and ^{18}O.

	H, T	T_p, K	ΔT_{isot} [a]	ΔT_p [b]	$T_{MR_{max}}$, K	MR_{max}, 10^2	W_p, meV [c]	A, 10^{-4} mΩ cm/K [c]
LPCM	0	181		0				
on LAO,	1	206	136	25	169	0.5	134 ± 2	3.55 ± 0.1
^{16}O	2	219	101	38	173	1.1		
	3	228	96	47	177	1.5		
LPCM	0			0			154 ± 2	
on LAO,	1	70						2.8 ± 0.5
^{18}O	2	118		47				
	3	132		62		$> 10^4$		
LPCM	0	186	63	0				
on STO,	1	202	46	16	173	0.02	137 ± 2	6.45 ± 0.1
^{16}O	2	209	34	23	175	0.005		
	3	220	31	33	175	0.1		
LPCM	0	123		0				
on STO,	1	156		33	117	1.0	145 ± 2	6.4 ± 0.5
^{18}O	2	175		52	120	2.7		
	3	189		65	120	5.0		

[a] $\Delta T_{isot} = T_p(^{18}O) - T_p(^{16}O)$.
[b] $\Delta T_p = T_p(H) - T_p(0)$.
[c] $\rho = AT \exp(W_p/kT)$.

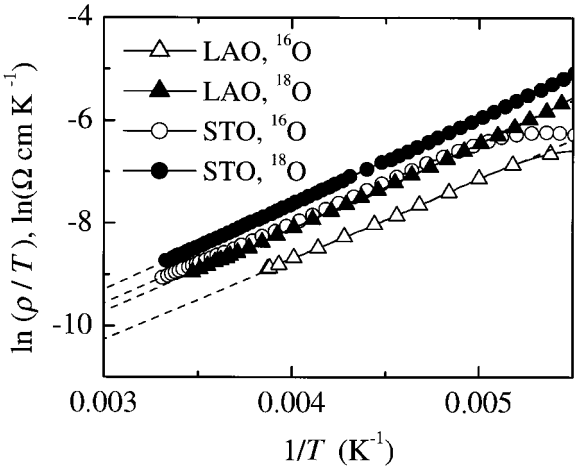

Fig. 4. Resistivity ρ/T *versus* inverse temperature for epitaxial $La_{0.35}Pr_{0.35}Ca_{0.3}MnO_3$ films on $LaAlO_3$ (LAO) and $SrTiO_3$ (STO) substrates annealed in ^{16}O and ^{18}O. Dashed lines are fits to the polaron model, see equation (1), solid lines are connecting the experimental data points and are guides to eyes.

where W_p is the small polaron hopping energy. This expression was used to find the effective activation energy from the experimental data in the high-temperature region. The values of W_p and of factor A were determined using the ρ/T *versus* $1/T$ plot (see Fig. 4). The obtained values for all samples under study (see Tab. 2) agree well with the data reported for $La_{0.7}Ca_{0.3}MnO_3$ [26,27]. The data presented in Table 2 demonstrate that both for films on LAO and STO $^{16}O \rightarrow {}^{18}O$ isotope substitution results in certain growth of W_p (see also [28]). This gives additional indications of the tendency to enhanced charge localization in the case of heavier isotope, which eventually manifests itself at lower temperatures in the isotope-driven metal-insulator transition discussed above. Unfortunately, the accuracy in determining A is not sufficient to make definite conclusions concerning the isotope mass dependence of this parameter and its relation to W_p. Nevertheless, the smaller values of A for ^{16}O are in agreement with the results reported in [19,28].

3.4 ac magnetic susceptibility

The electrical resistivity data for $La_{0.35}Pr_{0.35}Ca_{0.3}MnO_3$ films correlate with the behavior of the real part of ac magnetic susceptibility χ' measured at 4.2−300 K (see Fig. 5). The form of $\chi'(T)$ curves for the films on LAO annealed in ^{16}O is characteristic of the ferromagnetic ordering with the small admixture of the antiferromagnetic phase (small hysteresis of $\chi'(T)$ curves). After annealing in ^{18}O, the magnitude of $\chi'(T)$ decreases dramatically suggesting nearly complete transition of the compound to the antiferromagnetic state. For the films on STO, the annealing in ^{18}O affects only slightly the behavior of $\chi'(T)$. A small decrease in $\chi'(T)$ is observed for the samples with ^{18}O suggesting a certain lowering in the degree of ferromagnetic ordering in these samples.

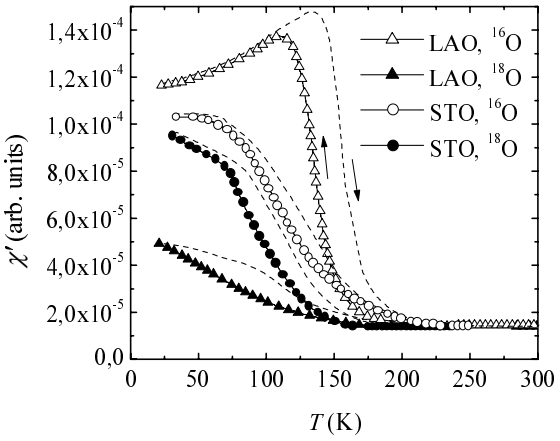

Fig. 5. Temperature dependence of *ac* susceptibility for $La_{0.35}Pr_{0.35}Ca_{0.3}MnO_3$ films with ^{16}O and ^{18}O on $LaAlO_3$ (LAO) and $SrTiO_3$ (STO) substrates. Dashed lines correspond to the heating runs.

4 Discussion

The study of oxygen $^{16}O \rightarrow {}^{18}O$ isotope substitution in $(La_{0.5}Pr_{0.5})_{0.7}Ca_{0.3}MnO_3$ thin films revealed a significant difference in the properties of the films deposited on LAO and STO substrates. The low-temperature metal-insulator transition was observed for the films on LAO substrate after the isotope substitution, while for the films on STO substrate, we have a large (about 60 K) shift of T_p (Fig. 2). Such an unusual difference in electrical properties can be explained by additional strains induced by substrates. The lattice constant of LAO is less than that in the manganites under study, and the lattice constant of STO is larger than in these manganites. Therefore, the crystal lattice is strained in both cases and this affects the electrical transport in the films under study.

In fact, the localization of itinerant electrons implies a narrowing of the conduction band. The value of the conduction bandwidth W depends on the cosine of the Mn-O-Mn bond angle. At a certain critical value of the bond angle, the charge carriers become localized. If W is about the corresponding cut-off value, then even an anisotropic perturbation of the bond angles in the structure caused by the lattice strain would result in a dramatic variation of sensitivity to the oxygen isotope mass. Because of the strain, the film on LAO is actually closer to the critical state for the localization of itinerant carries than the film on STO. Actually, the strain causes the increase in the Mn-O-Mn bond angles in the plane of the film on STO. On the contrary, in the plane of the film on LAO the Mn-O-Mn bond angles are decreased.

The in-plane contraction of the thin film deposited onto the LAO substrate shifts the crossover from the metal-like to the charge ordered state toward smaller y values resulting in the metal-insulator transition at $y = 0.5$. For ceramic samples this transition takes place at $y = 0.75$. Thin $(La_{1-y}Pr_y)_{0.7}Ca_{0.3}MnO_3$ films on STO substrates have a positive sign of the strains (stretching in the substrate plane). The Mn-O-Mn bond angle grows, distortions become smaller and the films remain metallic after the $^{16}O \rightarrow {}^{18}O$ substitution, although they exhibit a pronounced isotope shift of the resistivity peak.

These considerations are supported by variation of T_p for $(La_{1-y}Pr_y)_{0.7}Ca_{0.3}MnO_3$ films as a function of y: owing to the decrease of the mean value of the Mn-O-Mn bond angle, T_p decreases with growth of y but more rapidly for the films on LAO than for those on STO [29]. For comparison, the mean values of the Mn-O-Mn bond angle for $La_{0.7}Ca_{0.3}MnO_3$ with $T_p \approx 260$ K is 160 degrees and for the charge-ordered insulator $Pr_{0.7}Ca_{0.3}MnO_3$ we have 156 degrees [30]. From trivial geometry consideration, the tetragonal strain of 1% is equivalent of approximately 0.5 degree perturbation for such a Mn-O-Mn bond angle in the film plane.

As a result, the films on LAO are closer to the critical Mn-O-Mn angle corresponding to localization of carriers and the magnetic field produces a larger effect on mobility of the charge carriers in these films than in the films on STO. This implies larger values of *MR* for the films on LAO.

The possibility for localization of itinerant carries in films on LAO is related to the fact that this system is close to the crossover between the charge ordered antiferromagnetic insulator and ferromagnetic metal states that manifests itself in the behavior of susceptibility in these films. The vicinity of this phase boundary underlies also a pronounced temperature hysteresis of resistivity for the film on LAO, which is a general signature of the first order phase transitions and of the phase separation accompanying them. The existence of a magnetic first order transition usually gives an indication of the coupling between the spin subsystem and lattice distortions, inhomogeneous electron density distribution, or some other types of ordering. The interrelation between the magnetic and charge ordering (or within a more general approach, between spin, electron, and lattice subsystems) should favor the temperature hysteresis, and the width of hysteresis loops indirectly characterizes the strength of the corresponding coupling. Thus, the significant isotope effect in the width of hysteresis loops demonstrates an important role of the electron-lattice coupling in manganites, which is additionally enhanced in the vicinity of the FM-CO phase boundary.

5 Conclusion

The isotope effect for thin films on different substrates is a unique tool to study the role of magnetic ordering, charge ordering, and phase separation in manganites. The change in the lattice strains alongside with variation of composition in $(La_{1-y}Pr_y)_{0.7}Ca_{0.3}MnO_3$ thin film provides an opportunity for fine tuning the parameters of the materials near the crossover between ferromagnetism and charge ordering. Near this crossover the system turns out to be most sensitive to isotope substitution, which reveals the relative role of competing order parameters. $La_{0.35}Pr_{0.35}Ca_{0.3}MnO_3$ epitaxial thin films deposited onto both $LaAlO_3$ and $SrTiO_3$ substrates are in the vicinity

of this crossover and demonstrate a huge isotope effect. However, the films on $LaAlO_3$, appear to be so close to the phase boundary that $^{16}O \rightarrow {}^{18}O$ isotope substitution leads to the metal-insulator transition, phase separation phenomena, and a unique sensitivity of transport properties to the applied magnetic field.

We are grateful to A.N. Taldenkov, A.V. Inyushkin, A.A. Nikonov, and S.Yu. Shabanov for helpful assistance. The work was supported by INTAS (projects 97-0963 and 97-11954) and by Russian-Dutch Program for Scientific Cooperation.

References

1. C.N.R. Rao, A.K. Cheetham, R. Mahesh, Chem. Mater. **8**, 2421 (1996).
2. A.P. Ramirez, J. Phys. Cond. Matt. **9**, 8171 (1997).
3. H.W. Hwang, S.-W. Cheong, P.G. Radaelli, M. Marezio, B. Batlogg, Phys. Rev. Lett. **75**, 914 (1995).
4. J.M. de Teresa, M.R. Ibarra, J. Garsia, J. Blasco, C. Ritter, P.A. Algarabel, C. Marguina, A. del Moral, Phys. Rev. Lett. **76**, 3392 (1996).
5. A. Moreo, S. Yunoki, E. Dagotto, Science **283**, 2034 (1999).
6. A.J. Millis, Nature (London) **392**, 147 (1998).
7. T.A. Tyson, J. Mustre de Leon, S.D. Conradson, A.R. Bishop, J.J. Neumeier, H. Roeder, J. Zang, Phys. Rev. B **53**, 13985 (1996).
8. D. Louca, T. Egami, E.L. Brosha, H. Roeder, A.R. Bishop, Phys. Rev. B **56**, 8475 (1997).
9. P. Dai, J. Zhang, H.A. Mook, S.H. Liou, P.A. Dowben, E.W. Plummer, Phys. Rev. B **54**, 3694 (1996).
10. G.M. Zhao, K. Conder, H. Keller, K.A. Müller, Nature (London) **381**, 676 (1996).
11. G.M. Zhao, H. Keller, A. Shengelaya, K.A. Müller, Solid State Commun. **104**, 57 (1997).
12. N.A. Babushkina, L.M. Belova, O.Yu. Gorbenko, A.R. Kaul, A.A. Bosak, V.I. Ozhogin, K.I. Kugel, Nature (London) **391**, 159 (1998).
13. N.A. Babushkina, L.M. Belova, V.I. Ozhogin, O.Yu. Gorbenko, A.R. Kaul, D.I. Khomskii, K.I. Kugel, J. Appl. Phys. **83**, 7369 (1998).
14. I. Isaac, J.P. Franck, Phys. Rev. B **57**, R5602 (1998).
15. N.A. Babushkina, L.M. Belova, A.N. Taldenkov, E.A. Chistotina, D.I. Khomskii, K.I. Kugel, O.Yu. Gorbenko, A.R. Kaul, J. Phys. Cond. Matt. **11**, 5865 (1999).
16. A.M. Balagurov, V.Yu. Pomjakushin, D.V. Sheptyakov, V.L. Aksenov, N.A. Babushkina, L.M. Belova, A.N. Taldenkov, A.V. Inyushkin, P. Fischer, M. Gutmann, L. Keller, O.Yu. Gorbenko, A.R. Kaul, Phys. Rev. B **60**, 383 (1999).
17. O.Yu. Gorbenko, A.R. Kaul, N.A. Babushkina, L.M. Belova, B. Güttler, Austr. J. Phys. **52**, 269 (1999).
18. L.M. Belova, N.A. Babushkina, O.Yu. Gorbenko, A.R. Kaul, D.I. Khomskii, K.I. Kugel, J. Supercond. **12**, 269 (1999).
19. G.M. Zhao, Y.S. Wang, D.J. Kang, W. Prellier, M. Rajeswari, H. Keller, T. Venkatesan, C.W. Chu, R.L. Greene, Phys. Rev. B **62**, R11949 (2000), `cond-mat/9912355`.
20. J.N. Eckstein, I. Bozovic, J. O'Donnel, M. Onellion, M.S. Rzchowski, Appl. Phys. Lett. **69**, 1312 (1996).
21. O.Yu. Gorbenko, N.A. Babushkina, L.M. Belova, A.A. Bosak, V.A. Amelichev, A.R. Kaul, G. Wahl, in *Proceedings of the XIVth International Conference on CVD and EuroCVD-11, 1997*, Electrochemical Society Proceedings **97-25**, edited by M.D. Allendorf, C. Bernard (Electrochemical Society Inc., Pennington, 1997), p. 1101.
22. O.Yu. Gorbenko, V.N. Fuflyigin, Y.Y. Erokhin, I.E. Graboy, A.R. Kaul, Yu.D. Tretyakov, G. Wahl, L. Klippe, J. Mater. Chem. **4**, 1585 (1994).
23. B.A. van Hassel, T. Kawada, N. Sakai, H. Yokokawa, M. Dokiya, H.J.M. Bouvmeester, Solid State Ionics **66**, 295 (1993).
24. B. Güttler, L. Skuja, O.Yu. Gorbenko, A.R. Kaul, M.A. Novozhilov, N.A. Babushkina, L.M. Belova, in *High density magnetic recording and integrated magneto-optics*, MRS Proceedings **517**, edited by J. Bain, M. Levy, J. Lorenzo, T. Nolan, Y. Okamura, K. Rubin, B. Stadler, R. Wolfe (Material Research Society, Warrendale, Pennsylvania, 1998), p. 111.
25. D. Emin, T. Holstein, Ann. Phys. (N. Y.) **53**, 439 (1969).
26. M. Ziese, C. Srinitiwarawong, Phys. Rev. B **58**, 11519 (1998).
27. J.M. de Teresa, K. Dorr, K.H. Muller, L. Schultz, R.I. Chakalova, Phys. Rev. B **58**, R5928 (1998).
28. J.P. Franck, I. Isaac, Weimin Chen, J. Chrzanowski, J.C. Irwin, Phys. Rev. B **58**, 5189 (1998).
29. O.Yu. Gorbenko, A.A. Bosak, A.R. Kaul, N.A. Babushkina, L.M. Belova, in *Chemical Aspects of Electronic Ceramics Processing*, MRS Proceedings **495**, edited by P.N. Kumta, A.F. Hepp, D.B. Beach, B. Arkles, J.J. Sullivan (Material Research Society, Warrendale, Pennsylvania, 1998), p. 333.
30. P.G. Radaelli, G. Iannone, M. Marezio, H.Y. Hwang, S.-W. Cheong, J.D. Jorgensen, D.N. Argyriou, Phys. Rev. B **56**, 8265 (1997).